

Article

Evolution of Uranium Isotopic Compositions of the Groundwater and Rock in a Sandy-Clayey Aquifer

Alexander I. Malov 

Federal Center for Integrated Arctic Research of Russian Academy of Sciences, Arkhangelsk 163000, Russia; malovai@yandex.ru; Tel.: +7-911-571-7172

Received: 4 October 2017; Accepted: 20 November 2017; Published: 23 November 2017

Abstract: Uranium isotopes have been used as mechanistic or time scale tracers of natural processes. This paper describes the occurrence and redistribution of U in the Vendian aquifer of a paleo-valley in NW Russia. Forty-four rock samples were collected from nine boreholes with depths up to 160 m, and 25 groundwater samples were collected from 23 boreholes with depths up to 300 m. The U, Fe concentration, and $^{234}\text{U}/^{238}\text{U}$ activity ratio were determined in the samples. Estimations were made of the ^{14}C and ^{234}U - ^{238}U residence time of groundwater in the aquifer. It has been established that the processes of chemical weathering of Vendian deposits led to the formation of a strong oxidation zone, developed above 250 m.b.s.l. The inverse correlation between the concentrations of uranium and iron is a result of removal of U from paleo-valley slopes in oxidizing conditions, accumulation of U at the bottom of the paleo-valley in reducing conditions, and accumulation of Fe on the slopes and removal from the bottom of the paleo-valley. Almost all U on the slopes has been replaced by a newly formed hydrogenic U with a higher $^{234}\text{U}/^{238}\text{U}$ activity ratio. After, dissolution and desorption of hydrogenic U occurred from the slopes during periods with no glaciations and marine transgressions. Elevated concentrations of U are preserved in reduced lenses at the paleo-valley bottom. In these areas, the most dangerous aspect is the flow of groundwater from the underlying horizons, since during the operation of water supply wells it can lead to the creation of local zones of oxidizing conditions in the perforated screens zone and the transition of uranium into solution. For groundwater under oxidizing conditions, an increase in the concentration of uranium is characteristic of an increase in the residence time (age) of water in the aquifer. Also, the $^{234}\text{U}/^{238}\text{U}$ activity ratio increases with increasing radioactivity of groundwater. Therefore, the most rational approach is to use groundwater for drinking water supply from the slopes of the Northern Dvina basin.

Keywords: aquifer; rock; radioactive isotopes; groundwater dating; radioactivity of groundwater

1. Introduction

It is not uncommon for uranium isotopes to be used as mechanistic or time scale tracers of natural processes [1,2]. Uranium isotopes may be applied to determine the radiological suitability of groundwater for drinking purposes [3–6], applied in ore bodies exploration [7–9], or applied to assist in understanding historical climates [10–12]. Of special interest is the study of the uranium redistribution in the sandstones and siltstones of aquifers of paleo-valleys, which are associated with the formation of increased concentrations of uranium in both rocks and in groundwater [13]. A typical area with similar conditions is the Northern Dvina basin (NDB)—a paleo-valley in NW Russia ($39^{\circ}30'–41^{\circ}57'$ E and $64^{\circ}06'–64^{\circ}48'$ N) (Figure 1). The large industrial and urban agglomeration of Arkhangelsk–Severodvinsk–Novodvinsk is on this territory, and its water supply is currently affected using surface water. Groundwater has the best quality, but the rationale for the radiological safety of its use is required.

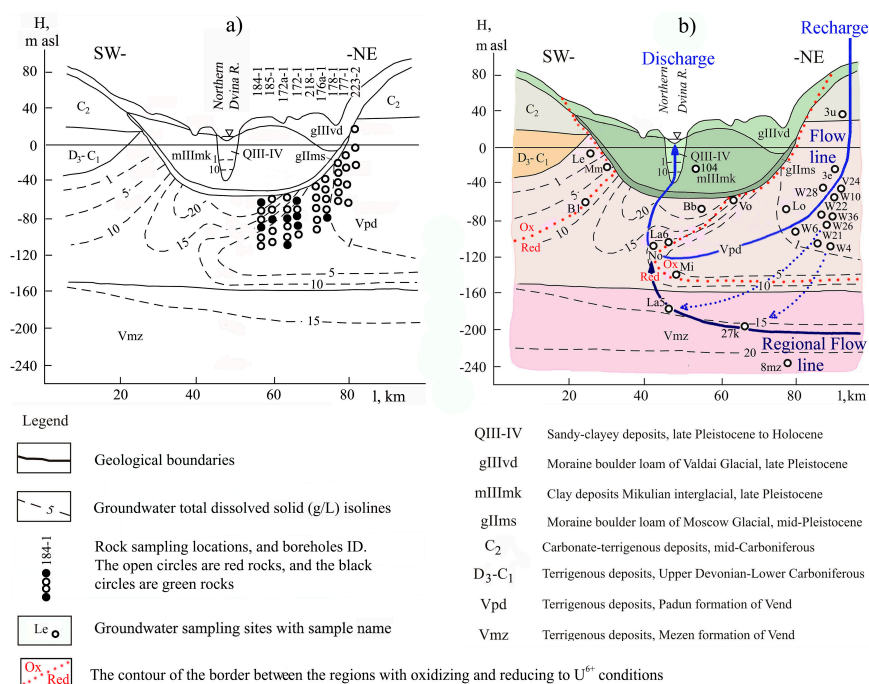


Figure 1. General location of the study site showing (a) the rock sampling locations and (b) the groundwater sampling locations on a conceptual schematic cross-section of the groundwater system perpendicular to the main axis of the Northern Dvina basin from the recharge area to the discharge in the river valley, including the location of the flow path of the water body in the aquifer.

The aim of this paper is to carry out the paleoreconstruction of hydrodynamics of NDB with an assessment of the direction of the evolution of the uranium-isotope composition of rocks and groundwater during the Pleistocene-Holocene transition.

The following questions are of interest:

What trends are observed in the evolution of the uranium-isotopic composition of rocks?

Uranium almost completely transfers into the groundwater from water-bearing sediments via cracks and pores, through which water moves from recharge to discharge areas. Where are the maximum concentrations of uranium located in the water bearing rocks and how widely are they developed?

When the operation of water supply wells is carried out it can lead to upwelling water with higher radioactivity from the underlying horizons. On which sections of the NDB is it the most dangerous with respect to upwelling water?

The impact of uranium on water quality is determined by its concentration (chemical aspect) and isotopes activity (radiological aspect). How does the residence time (age) of groundwater in the aquifer influence on its radioactivity?

2. Materials and Methods

The object of this study is the Padun aquifer of the NDB. The Northern Dvina basin represents an onshore continuation of the Dvina Bay of the White Sea. It has been formed in the sequence of sediments with different ages, namely, the Middle Carboniferous carbonate-terrigenous (C₂), Upper Devonian-Lower Carboniferous terrigenous (D₃-C₁), and Vendian Padun (Vpd) and Mezen (Vmz) Formations (Figure 1).

The NDB is 120 km long. Maximal dimension of its transverse section (along the coast of the Dvina Bay) is as follows: width of the top zone is 100–110 km, width of the bottom is 30–40 km. The bottom is located at 60 m below sea level (m.b.s.l) and the slopes are inclined at an angle of 2–3°.

The basin is largely filled with clayey sediments from the Mikulinian interglacial (mIIIImk) Boreal sea. The clays are underlain by a 10 to 15 m-thick sequence of loams from the Moskovian moraine (gIIIm). The underlying Vendian terrigenous sequence (600–700 m) is composed of alternating sandstones, siltstones, and mudstones. The Mikulinian clays are overlain by a 10 to 15 m-thick sequence of Valdaian glaciation (gIIIvd) sediments, which are largely represented by moraine boulder loams with local fluvioglacial and glaciolacustrine sands. The valley of the Northern Dvina River is filled with Upper Pleistocene and Holocene (QIII-IV) sandy clay sediments.

The upper part of the Vendian aquifer in the central part of the depression is characterized by inversion type of vertical hydrochemical zonality and decreasing groundwater mineralization from 29 to 12 g·L⁻¹ (Figure 1). This pattern is primarily caused by the freshening of groundwater due to the long-term existence of terrestrial conditions during the Mesozoic and Cenozoic. The desalination of groundwater ceased after the Mikulino Sea transgression ~130 ka ago. Subsequently, the upper part of the Vendian aquifer began to receive saline interstitial water, which was squeezed out under the load of the Valdai glacier from Mikulinian interglacial marine clays. After the formation of the Northern Dvina River valley due to the erosional activity of water that flowed from the melting glacier, the valley cut the Mikulinian clayey sequence almost to its base. Saline water from the aquifer sediments of the terrigenous Padun Formation began to flow into the river valley and were later replaced by freshwater from the recharge area (Figure 1).

Sediments of the Padun Formation of the study area were accumulated in the coastal marine environment. The Padun Formation of the Vend is 90–170 m thick and located above 150 m.b.s.l. It is composed of siltstones and sandstones with intercalations of mudstones. The rocks are characterized by reddish brown color on the NDB slope with light green lenses and spots the under central part of the NDB (at the NDB bottom).

Forty-four rock samples were collected from 9 boreholes down to depths of 160 m, and 25 groundwater samples from 23 boreholes of depths up to 300 m (Figure 1; Tables 1 and 2).

Table 1. Uranium content and ²³⁴U/²³⁸U activity ratio in the rocks of the Vendian (Ediacaran) Padun (Vpd) Formation at the Northern Dvina basin (NDB).

Well ID	Rock ^a	Depth (m)	²³⁸ U (ppm)	²³⁴ U/ ²³⁸ U (Bk/Bk)	Well ID	Rock	Depth (m)	²³⁸ U (ppm)	²³⁴ U/ ²³⁸ U (Bk/Bk)
Samples taken from rocks under the central part of the NDB (NDB Bottom)					Samples taken from rocks on the slope of the NDB (NDB Slope)				
184-1	GSi	106.0	3.15 ± 0.33	0.65 ± 0.10	218-1	RSi	72.8	1.02 ± 0.19	1.12 ± 0.19
	RSi	116.4	1.13 ± 0.22	1.17 ± 0.17		RM	82.5	1.26 ± 0.21	1.19 ± 0.20
	RSi	127.2	1.92 ± 0.36	1.09 ± 0.15		RSa	89.4	1.16 ± 0.18	1.23 ± 0.21
	GSi	127.2	20.9 ± 3.52	0.54 ± 0.08		RSi	108.1	0.63 ± 0.11	1.07 ± 0.18
	RSi	143.2	0.86 ± 0.15	1.21 ± 0.18		RSi	114	0.81 ± 0.14	1.34 ± 0.21
	RSi	156.0	0.63 ± 0.11	1.14 ± 0.16	176a-1	RSa	68.5	1.01 ± 0.16	1.50 ± 0.25
185-1	RSi	122.8	0.80 ± 0.14	1.21 ± 0.18		RSi	72.1	1.70 ± 0.26	1.13 ± 0.19
	RSi	133.0	0.68 ± 0.11	0.81 ± 0.12		RSi	85.6	1.69 ± 0.25	1.02 ± 0.18
	GM	144.1	1.52 ± 0.28	1.03 ± 0.15		RM	97.0	1.20 ± 0.19	1.26 ± 0.20
	VSi	153.4	2.16 ± 0.37	1.21 ± 0.18		GM	97.0	3.45 ± 0.48	1.18 ± 0.19
	RSi	160.0	0.11 ± 0.03	0.99 ± 0.15	177-1	RSS	52.0	0.58 ± 0.12	1.30 ± 0.21
172a-1	RSS	110.6	0.76 ± 0.13	0.99 ± 0.15		RSi	60.8	1.03 ± 0.16	1.33 ± 0.22
	VSi	120.0	1.11 ± 0.22	1.30 ± 0.19		RSi	78.1	1.79 ± 0.27	1.17 ± 0.19
	GSi	133.6	4.96 ± 0.75	1.21 ± 0.18		RM	89.0	1.26 ± 0.21	1.07 ± 0.18
	RSi	133.6	1.14 ± 0.23	1.12 ± 0.16	178-1	RSi	72.5	1.50 ± 0.23	1.07 ± 0.18
	RSi	150.9	1.45 ± 0.27	1.18 ± 0.17		RSa	79.4	1.74 ± 0.27	1.17 ± 0.19
	GSi	150.9	14.9 ± 2.31	0.77 ± 0.11		RSi	83.0	0.85 ± 0.15	1.21 ± 0.21
172-1	GSi	114.0	1.46 ± 0.23	1.07 ± 0.15		RSa	92.0	1.73 ± 0.27	1.13 ± 0.18
	RSi	119.6	1.57 ± 0.25	0.97 ± 0.15		RSa	101.5	0.84 ± 0.15	1.25 ± 0.20
	GSi	119.6	3.11 ± 0.38	0.93 ± 0.14	223-2	RSi	49.0	2.89 ± 0.78	1.51 ± 0.25
	GSi	131.6	2.10 ± 0.35	0.90 ± 0.14		RSi	70.0	0.83 ± 0.15	1.16 ± 0.19
	RSi	145.0	1.11 ± 0.22	1.12 ± 0.16		RSi	92.0	1.01 ± 0.17	1.05 ± 0.17
Average			3.07 ± 0.50	1.03 ± 0.16	Average			1.36 ± 0.23	1.20 ± 0.20
			Total average ²³⁸ U = 2.22 ± 0.36 ppm, ²³⁴ U/ ²³⁸ U = 1.12 ± 0.18						
			Green rock average ²³⁸ U = 6.17 ± 0.99 ppm, ²³⁴ U/ ²³⁸ U = 0.92 ± 0.15						
			Red rock average ²³⁸ U = 1.20 ± 0.20 ppm, ²³⁴ U/ ²³⁸ U = 1.16 ± 0.19						

Note: ^a GSi—green siltstones, RSi—red siltstones, GM—green mudstones, RM—red mudstones, VSi—variegated siltstones, RSS—red siltstone-sandstone, RSa—red sandstones.

Table 2. Measured values of the chemical and isotopic compositions of the groundwater and the calculated values of the ^{14}C and U ages (modified after [14]).

Sample Name	TDS (mg/L)	pH	DO (mg/L)	T (°C)	^{14}C (pmc)	$\delta^{13}\text{C}$ (‰)	Age (ka)	Eh (mV)	Alkalinity (meq/L)	Fe ($\mu\text{g/L}$)	C_8^{W} (ppb)	AR_t (Bk/Bk)
Samples taken from groundwater under the central part of the NDB (NDB Bottom)												
8mz ²⁰¹⁴	22,246	7.6	0	6.7	0	7.6	460 ± 70 ^b	NA	0.16	8097	0.2 ± 0.004	2.97 ± 0.45
27 ²⁰¹²	15,724	7.9	1.1	5.9	NA	NA	160 ± 25 ^c	−23	0.92	826	1.39 ± 0.03	5.45 ± 0.81
La5 ²⁰¹²	15,158	9	0	6.8	NA	NA	110 ± 17 ^c	−151	0.15	6031	0.12 ± 0.002	6.19 ± 0.93
La6 ²⁰¹²	9065	8.4	0.3	6.3	NA	NA	90 ± 15 ^c	−42	0.7	708	0.47 ± 0.01	6.53 ± 0.98
No ²⁰¹⁴	8954	8.3	1.2	6.8	0	NA	80 ± 14 ^c	−82	0.57	1352	0.28 ± 0.01	6.72 ± 1.05
Bb ²⁰⁰³	20,619	NA	NA	NA	NA	NA	NA	NA	3.97	400	NA	NA
B1 ²⁰¹²	8399	7.7	1.2	5.7	5.78 ± 0.24	−16.6	27.3 ± 0.6 ^a	−38	4.18	1872	15.22 ± 0.3	5.46 ± 0.82
B1 ²⁰¹⁴	9193	7.6	NA	5.8	5.79 ± 0.19	−15.6	26.1 ± 0.6 ^a	NA	4.07	776	15.38 ± 0.3	5.41 ± 0.81
Vo ²⁰¹²	13,370	7.7	0	5.3	NA	NA	22.2 ± 3.3 ^b	NA	2.18	NA	13.84 ± 0.3	4.75 ± 0.71
Mi ²⁰¹⁴	5317	7.4	0	5	1.70 ± 0.26	−14.6	33.0 ± 2.3 ^a	−25	1.74	439	9.86 ± 0.2	7.16 ± 0.94
MM ²⁰¹²	4362	7.8	NA	4.8	NA	NA	16.6 ± 2.4 ^b	2	3.75	443	7.24 ± 0.14	6.4 ± 0.96
Samples taken from groundwater on the slope of the NDB (NDB Slope)												
3e ²⁰¹⁵	138	8.7	3.5	4.8	34.18 ± 0.59	−12.3	2.1 ± 0.3 ^a	−68	1.62	203	12.15 ± 0.24	2.26 ± 0.34
W10 ²⁰¹⁴	387	9.1	1.4	4.1	NA	NA	11.7 ± 1.8 ^b	101	3.67	5.6	11.22 ± 0.22	2.39 ± 0.36
W6 ²⁰¹⁴	738	8.9	0.6	4.5	25.30 ± 0.64	−9.6	4.0 ± 0.3 ^a	99	3.75	9.5	5.21 ± 0.92	2.86 ± 0.42
W21 ²⁰¹⁴	647	8.6	2.9	4.6	NA	NA	4.8 ± 0.8 ^b	23	3.44	18.2	7.55 ± 0.15	1.99 ± 0.3
W4 ²⁰¹²	638	9	0	4.7	NA	NA	16.4 ± 2.4 ^b	106	3.97	3.9	7.0 ± 0.14	4.76 ± 0.72
V24 ²⁰¹²	307	8.6	1.5	3.8	NA	NA	8.9 ± 1.4 ^b	−12	3.33	71.9	5.71 ± 0.11	3.51 ± 0.52
3u ²⁰¹⁴	285	7.7	NA	4.0	44.97 ± 1.08	−8.7	1.3 ± 0.2 ^b	NA	3.21	65.7	4.01 ± 0.84	1.46 ± 0.22
3u ²⁰¹⁵	93	7.8	NA	4.9	NA	NA	NA	NA	1.02	94.9	0.25 ± 0.01	1.28 ± 0.21
W22 ²⁰¹⁴	383	8.4	1.2	4.1	24.86 ± 0.43	−10.1	4.6 ± 0.4 ^a	−8	3.02	14.3	6.37 ± 0.13	1.63 ± 0.24
W28 ²⁰¹⁴	260	8.2	3.3	3.9	58.40 ± 0.89	−11.0	2.0 ± 0.3 ^b	106	3.05	9.3	2.99 ± 0.06	2.39 ± 0.36
W26 ²⁰¹⁴	365	8.1	0.8	4.4	NA	NA	2.8 ± 0.4 ^b	−34	3.61	10.8	2.38 ± 0.05	3.04 ± 0.45
W36 ²⁰¹⁴	348	8.2	2.7	5.2	25.01 ± 0.47	−11.7	5.8 ± 0.4 ^a	−62	3.56	59.1	2.0 ± 0.04	4.81 ± 0.62
Lo ²⁰¹⁴	790	9.0	1.8	4.7	37.03 ± 0.67	−11.2	5.4 ± 0.8 ^b	NA	5.25	26.4	1.78 ± 0.04	5.94 ± 0.84
Le ²⁰¹²	209	8.2	6	5	51.67 ± 0.63	−11.5	0.3 ± 0.05 ^b	−24	2.61	165	1.70 ± 0.03	1.43 ± 0.21

Note: NA not analyzed; NC not calculated. ^a ^{14}C age, ^b ^{234}U - ^{238}U age, ^c ^{234}U - ^{238}U age of the regional and local flow systems mix of groundwater (see Figure 1).

Water temperature, pH, Eh, DO, alkalinity, total dissolved solids (TDS), Fe concentrations, U concentrations (C_8^W), $^{234}\text{U}/^{238}\text{U}$ activity ratio (AR_t), ^{14}C , $\delta^{13}\text{C}$ were determined in groundwater, as described by Malov [14]. U content (^{238}U), $^{234}\text{U}/^{238}\text{U}$ activity ratio, Fe content in rock samples were determined, as described by Malov et al. [15].

A piston flow model was used to estimate the ^{14}C residence time of groundwater in the aquifer. The basic equation for groundwater dating is:

$$t = -\lambda_{14}^{-1} \ln(^{14}C_{DIC})(^{14}C_0)^{-1}$$

where t is the groundwater age, λ_{14} is the ^{14}C decay constant, $^{14}C_0$ is the ^{14}C after adjustment for the geochemical and physical processes in the aquifer (without radioactive decay), and $^{14}C_{DIC}$ is the measured ^{14}C value of the total dissolved inorganic carbon (TDIC) [16].

When analyzing the results of carbon isotope determinations, the following models were used to determine $^{14}C_0$: (1) for $\delta^{13}\text{C} < 0.5(\delta^{13}\text{C}_g + \delta^{13}\text{C}_s)$ —Mook model, taking into account the isotope exchange between soil CO_2 and TDIC (indices 'g' and 's' are soil CO_2 and solid carbonate minerals, respectively); (2) for $\delta^{13}\text{C} > 0.5(\delta^{13}\text{C}_g + \delta^{13}\text{C}_s)$ —Han and Plummer model, taking into account the isotope exchange between solid carbonates and TDIC.

Further, a mass-balance model [14,17] was used to estimate the ^{234}U - ^{238}U residence time of groundwater in an aquifer under oxidizing conditions for U.

The main calculated equations are as follows:

$$t = \ln(k^{-1})(\lambda_4)^{-1}, k = 1 - [C_8^W \cdot R \cdot (AR_t - 1)](M_s \cdot C_8^R \cdot p)^{-1}$$

where t is the groundwater residence time in an aquifer (age), λ_4 is the ^{234}U decay constant, C_8^W is the measured concentration of ^{238}U in solution at the point of sampling, R is the retardation factor, AR_t is the measured $^{234}\text{U}/^{238}\text{U}$ activity ratio in the pore fluid at the point of sampling, M_s is the solid mass to fluid volume ratio, C_8^R is the concentration of ^{238}U in solid phase, and p is the recoil loss factor. $k = e^{-\lambda_4 t} = 1 - \lambda_4 t (AR_t - 1)(AR_0 - 1)^{-1}$ [17], where AR_0 is the initial $^{234}\text{U}/^{238}\text{U}$ activity ratio in the pore fluid at the recharge area of the groundwater.

A model of the down-flow radioactive decay of ^{234}U excess in solution [18] was used to estimate the ^{234}U - ^{238}U residence time of groundwater in an aquifer under reducing conditions for U.

The main calculated equation is as follows [18]:

$$t = (R\lambda_4)^{-1} \ln(AR_0 - 1)(AR_t - 1)^{-1}$$

3. Results and Discussion

Groundwater on the NDB slope (Figure 2b,d; Table 2) represents fresh water. Their Eh ranges from -68 to 106 mV, pH from 7.7 to 9.1 and alkalinity from 1.0 to 5.2 meq/L. The residence time this water (age) ranged from 0.3 to 16.4 ka. Very low Fe concentration (4 – 203 , average 41 ppb), medium AR_t (1.3 – 5.9 , average 3.0) and high C_8^W (0.3 – 12.5 , average 5.4 ppb) are characteristic of this water. At the NDB bottom, near the redox barrier old salt water has ages ranging from 17 to 33 ka, TDS from 4 to 13 g/L, Eh from -38 to 2 mV, pH from 7.4 to 7.8 and alkalinity from 1.7 to 4.2 meq/L. Maximum C_8^W (7.2 – 15.4 , average 12 ppb), and high AR_t (4.8 – 7.2 , average 5.9) and Fe (0.4 – 1.9 , average 0.8 ppm) are observed here. Below the redox barrier exist the oldest (^{234}U - ^{238}U age from 0.1 to 0.5 Ma) and the most salty (TDS from 9 to 22 g/L) waters. The Eh ranged from -23 to -151 mV, pH ranged from 7.6 to 9 , alkalinity ranged predominantly from 0.2 to 0.9 meq/L. The minimum C_8^W (0.1 – 1.4 , average 0.4 ppb) and maximum Fe (0.7 – 8 , average 3.7 ppm) are observed here. AR_t decreases from 7.16 ± 0.94 to 2.97 ± 0.45 .

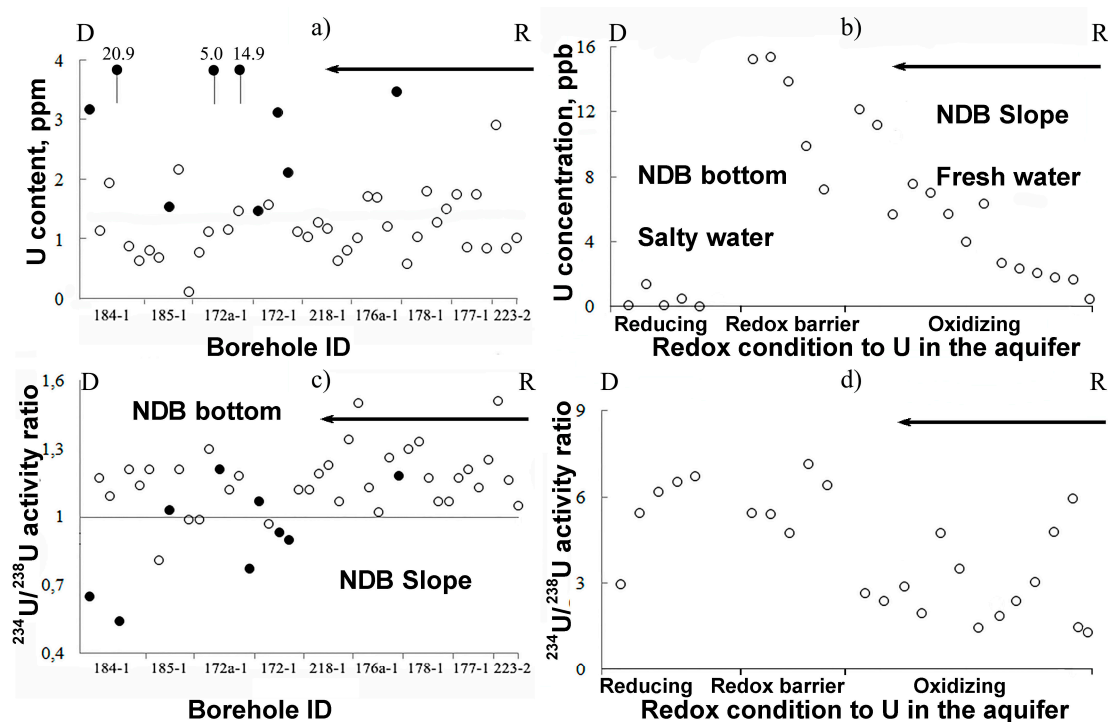


Figure 2. Uranium and its isotopes distribution in Padun aquifer of the NDB from the recharge area on the watershed to the NDB slope and NDB bottom and discharge in the river valley: red (empty circles) and green (solid circles) rock samples (a,c) and groundwater samples (b,d). Arrows indicate the direction of groundwater flow path and uranium redistribution. R—recharge area, D—discharge area.

Below the redox barrier, at the NDB bottom, the uranium becomes restored to U^{4+} and precipitates (Figure 2b), its concentration in rocks reaches 20 ppm, and $^{234}\text{U}/^{238}\text{U}$ activity ratio in rocks decreases to 0.5–0.9 (Figure 2a,c; Table 1). However, complete precipitation does not occur because the process of recoil loss continues and both isotopes of U enter into the water. For every 1 atom of ^{234}U in rock, ~18,000 atoms of ^{238}U exist; therefore, recoil atoms inevitably encounter and knock other atoms from the crystal lattice, creating an area of disorder. The uranium atoms in the disordered zone are first transferred to water, resulting in a disturbance of the radioactive equilibrium in the water. Evidence that recoil atoms are not transferred into water alone but carry away a certain amount of ^{238}U atoms explains why AR_t under reducing conditions usually does not exceed 10–20. This is possible if 1000–2000 ^{238}U atoms are transferred into the water with each recoil-atom ^{234}Th [14].

The maximum AR_t in groundwater directly close to the redox barrier is estimated to be 7.16 ± 0.94 (sample Mi²⁰¹⁴). In other samples, the activity ratio is lower, namely, from 6.72 ± 1.05 to 2.97 ± 0.45 (Figure 2d; Table 2), which suggests a greater age for the groundwater in these samples, in accordance with a simple model of the down-flow radioactive decay of excess ^{234}U in solution.

The U content in the red rock ranged from 0.11 ppm to 2.89 ppm, average 1.2 ppm (Table 1). The U content in the green rock ranged from 1.52 ppm to 20.9 ppm, average 6.17 ppm. $^{234}\text{U}/^{238}\text{U}$ activity ratio in the red rock ranged from 0.87 to 1.51, average 1.16. $^{234}\text{U}/^{238}\text{U}$ activity ratio in the green rock ranged from 1.18 to 0.54, average 0.92 ppm. The average value of U content on the slope of the NDB is 1.36 ppm, $^{234}\text{U}/^{238}\text{U}$ activity ratio is 1.2; at the bottom of the NDB average values are 3.07 and 1.03, respectively (Table 1; Figure 2b,d).

The average value of Fe content from 18 samples of red rocks on the slope of the NDB is 3.67%. In two samples from wells 184-1 on the NDB bottom Fe in the red rock is 2.33%, Fe in the green rock is 1.83%.

In Upper Vendian products of the rocks weathering were transferred to the study area from the nearby eastern tip of the Baltic Shield and were deposited together with buried organic matter. In subsequent geological periods (Upper Devonian–Lower Carboniferous) NDB was also in coastal marine and lake environments under a hot humid climate [19,20]. In such anoxic environments, early diagenesis conditions favor the reduction of U^{6+} into low solubility U^{4+} , which decreases U concentrations in overlying waters and sediment pore-waters [21]. This period was the most favorable for the supergene ore formation [22,23]. During these periods apparently this was the main flow of uranium to the study area and its deposition as a result of hydrolysis, adsorption on natural sorbents promoted changes in the oxidizing conditions of the environment in reducing conditions.

The transgressive period, in Middle Carboniferous–Permian led to the formation of a cover of the terrigenous-carbonate deposits (see Figure 1), however, during the long continental environmental interspace in the Mesozoic–Pliocene was formed the NDB palaeo valley. Its depth could reach 250–300 m. The depth of the valley and its Pliocene age are confirmed by the data of other paleovalleys of the East European platform [24–26]. Within its boundaries, most of the Paleozoic sediments were destroyed, and Vendian deposits were brought to the surface (see Figure 1).

The processes of chemical weathering of Vendian deposits led to the formation of a strong oxidation zone, developed above 250 m.b.s.l. The greater increase in the proportion of Fe^{2+} iron is typically the presence of bitumen, organic carbon, pyrite, and rock which maintain the gray-green color [27,28]. This period probably provided the main redistribution of uranium accumulated during the Paleozoic in the Padun aquifer of the NDB. The inverse correlation between the concentrations of uranium and iron is typical for Padun rock (see above). It is a result of removal of U from NDB slopes in oxidizing conditions and accumulation of U at the bottom of the NDB in reducing conditions, and accumulation of Fe on the slopes and removal from bottom. As a result, a significant part of the equilibrium U on the slopes of the NDB had been replaced by a newly formed “hydrogenic” U (precipitated from groundwater), with an initial $AR_0 \approx AR_t$ of modern fresh groundwater = 3, and the initial U content of the rocks (U_0) \approx U content of modern siltstones of the region (2.6 ppm). The ending of the period of co-precipitation of hydrogenic uranium with iron hydroxide on NDD slopes can be estimated from the equation [17]:

$$t_1 = \lambda_4^{-1} \ln \left[(AR_0 - 1)(AR_t - 1)^{-1} \right]$$

where $\lambda_4 = 2.8263 \times 10^{-6}$ (a^{-1}) [29]; AR_t is average $^{234}U/^{238}U$ activity ratio of the red rock = 1.16 (see Table 1).

What is obtained is: $t_1 = 0.9$ Ma, which should roughly correspond to the period of a sharp cold snap in the region and filling of the paleo-valley by clay material [30–33]. The duration of the subsequent removal of hydrogenic uranium from the NDD slopes can be estimated from the equation [14]:

$$t_2 = (C_8^W \cdot R)(R_d \cdot M_s \cdot C_8^R)^{-1}$$

where C_8^W —concentration of U that was passed from the red siltstones to the water for time t :

$$C_8^W = U_0 - ^{238}U$$

where $U_0 = 2.6$ ppm (see above) and ^{238}U is the red rock average ^{238}U content (1.2 ppm) (see Table 1). Consequently $C_8^W = (2.6 - 1.2) = 1.4$ ppm; M_s —solid mass to fluid unit volume ratio = 9.2; C_8^R is average concentration of U in solid phase for a time t : $C_8^R = (U_0 + ^{238}U) : 2 = (2.6 + 1.2) : 2 = 1.9$ ppm; R_d —dissolution rate for U; $R : p = 24$; and average $R_d : p = 3.6 \times 10^{-6} a^{-1}$ [14].

We get: $t_2 = 0.5$ Ma. The difference ($t_1 - t_2$) should roughly correspond to the duration of glaciations and marine transgressions in the past 0.9 Ma, when the movement of groundwater in the Padun aquifer was significantly delayed or even absent [34–37]. The removal of uranium was not apparent, but radioactive decay continued.

Lower values of average $^{234}\text{U}/^{238}\text{U}$ activity ratio in the green siltstones (0.92) (see Table 1) can be explained by the fact that these deposits have reached a steady state of the $^{234}\text{U}/^{238}\text{U}$ activity ratio that depends only on their size (the average grain size $d_p \approx 30 \mu\text{m}$) [38], because they were under reducing conditions over 1 Ma. A significantly higher content of uranium in them compared to red siltstones shows a considerable variability in the permeability values of the aquifer, whereby they were away from the paths of groundwater filtration and have retained uranium. A similar situation is typical for the preserved iodine water lens here (sample Bb²⁰⁰³), the source of which is the iodine-containing seaweed from the Mikulinian interglacial Boreal sea [39].

4. Conclusions

The processes of chemical weathering of Vendian deposits led to the formation of a strong oxidation zone, developed above 250 m.b.s.l. The inverse correlation between the concentrations of uranium and iron is a result of removal of U from NDB slopes in oxidizing conditions and accumulation of U at the bottom of the NDB in reducing conditions, and accumulation of Fe on the slopes and removal from bottom. Almost all the U on the slopes of the paleo-valley could be replaced by a newly formed hydrogenic U with a higher $^{234}\text{U}/^{238}\text{U}$ activity ratio.

Afterwards, dissolution and desorption of hydrogenic U occurred from the slopes of the paleo-valley during periods with no glaciations and marine transgressions. Elevated concentrations of U are preserved in reduced lenses at the NDB bottom. In these areas, the most dangerous is the upwelling of groundwater from the underlying horizons, since during the operation of water supply wells it can lead to the creation of local zones of oxidizing conditions in the perforated screens zone and the transition of uranium into the aqua solution.

For groundwater under oxidizing conditions, an increase in the concentration of uranium is characteristic of an increase in the residence time (age) of water in the aquifer. Also, the $^{234}\text{U}/^{238}\text{U}$ activity ratio increases, increasing the radioactivity of groundwater. Therefore, the most rational conclusion would be to aim at using the groundwater from the slopes of the NDB for drinking water supply.

Acknowledgments: This work was supported by the Federal Agency of Scientific Organizations (project No. 0409-2015-0134).

Conflicts of Interest: The authors declare no conflict of interest. The founding sponsors had no role in the design of the study; in the collection, analyses, or interpretation of data; in the writing of the manuscript, and in the decision to publish the results.

References

1. Porcelli, D. Investigating groundwater processes using U- and Th-series nuclides. *Radioact. Environ.* **2008**, *13*, 105–153.
2. Baskaran, M. *Handbook of Environmental Isotope Geochemistry*; Springer: Berlin/Heidelberg, Germany, 2011.
3. Dhaoui, Z.; Chkir, N.; Zouari, K.; Hadj Ammar, F.; Agoune, A. Investigation of uranium geochemistry along groundwater flow path in the Continental Intercalaire aquifer (Southern Tunisia). *J. Environ. Radioact.* **2016**, *157*, 67–76. [[CrossRef](#)] [[PubMed](#)]
4. Wang, F.; Tan, L.; Liu, Q.; Li, R.; Li, Z.; Zhang, H.; Hu, S.; Liu, L.; Wang, J. Biosorption characteristics of Uranium (VI) from aqueous solution by pollen pini. *J. Environ. Radioact.* **2015**, *150*, 93–98. [[CrossRef](#)] [[PubMed](#)]
5. Yi, Z.; Yao, J.; Chen, H.-L.; Wang, F.; Yuan, Z.; Liu, X. Uranium biosorption from aqueous solution onto *Eichhornia crassipes*. *J. Environ. Radioact.* **2016**, *154*, 43–51. [[CrossRef](#)] [[PubMed](#)]
6. Manickum, T.; John, W.; Terry, S.; Hodgson, K. Preliminary study on the radiological and physicochemical quality of the Umgeni Water catchments and drinking water sources in KwaZulu-Natal, South Africa. *J. Environ. Radioact.* **2014**, *137*, 227–240. [[CrossRef](#)] [[PubMed](#)]

7. Hall, S.M.; Mihalasky, M.J.; Tureck, K.R.; Hammarstrom, J.M.; Hannon, M.T. Genetic and grade and tonnage models for sandstone-hosted roll-type uranium deposits, Texas Coastal Plain. *Ore Geol. Rev.* **2017**, *80*, 716–753. [[CrossRef](#)]
8. Cuvier, A.; Panza, F.; Pourcelot, L.; Foissard, B.; Cagnat, X.; Prunier, J.; van Beek, P.; Souhaut, M.; Le Roux, G. Uranium decay daughters from isolated mines: Accumulation and sources. *J. Environ. Radioact.* **2015**, *149*, 110–120. [[CrossRef](#)] [[PubMed](#)]
9. Keatley, A.C.; Scott, T.B.; Davis, S.; Jones, C.P.; Turner, P. An investigation into heterogeneity in a single vein-type uranium ore deposit: Implications for nuclear forensics. *J. Environ. Radioact.* **2015**, *150*, 75–85. [[CrossRef](#)] [[PubMed](#)]
10. Dosseto, A.; Schaller, M. The erosion response to Quaternary climate change quantified using uranium isotopes and in situ-produced cosmogenic nuclides. *Earth-Sci. Rev.* **2016**, *155*, 60–81. [[CrossRef](#)]
11. Jamieson, R.A.; Baldini, J.U.L.; Brett, M.J.; Taylor, J.; Ridley, H.E.; Ottley, C.J.; Pruffer, K.M.; Wassenburg, J.A.; Scholz, D.; Breitenbach, S.F.M. Intra- and inter-annual uranium concentration variability in a *Belizean stalagmite* controlled by prior aragonite precipitation: A new tool for reconstructing hydro-climate using aragonitic speleothems. *Geochim. Cosmochim. Acta* **2016**, *190*, 332–346. [[CrossRef](#)]
12. Wang, Q.; Song, J.; Li, X.; Yuan, H.; Li, N.; Cao, L. Environmental evolution records reflected by radionuclides in the sediment of coastal wetlands: A case study in the Yellow River Estuary wetland. *J. Environ. Radioact.* **2016**, *162–163*, 87–96. [[CrossRef](#)] [[PubMed](#)]
13. International Atomic Energy Agency. *World Distribution of Uranium Deposits (UDEPO), with Uranium Deposit Classification*; IAEA-TECDOC-1629; IAEA: Vienna, Austria, 2009.
14. Malov, A.I. Estimation of uranium migration parameters in sandstone aquifers. *J. Environ. Radioact.* **2016**, *153*, 61–67. [[CrossRef](#)] [[PubMed](#)]
15. Malov, A.I.; Bolotov, I.N.; Pokrovsky, O.S.; Zykov, S.B.; Tokarev, I.V.; Arslanov, K.A.; Druzhinin, S.V.; Lyubas, A.A.; Gofarov, M.Y.; Kostikova, I.A.; et al. Modeling past and present activity of a subarctic hydrothermal system using O, H, C, U and Th isotopes. *Appl. Geochem.* **2015**, *63*, 93–104. [[CrossRef](#)]
16. Han, L.F.; Plummer, N. A review of single-sample-based models and other approaches for radiocarbon dating of dissolved inorganic carbon in groundwater. *Earth-Sci. Rev.* **2016**, *152*, 119–142. [[CrossRef](#)]
17. Malov, A.I. The use of the geological benchmarks to assess the residence time of groundwater in the aquifer using uranium isotopes on the example of the Northern Dvina basin. *Lithol. Miner. Resour.* **2013**, *48*, 254–265. [[CrossRef](#)]
18. Ivanovich, M.; Fröhlich, K.; Hendry, M.J. Uranium-series radionuclides in fluids and solids, Milk River aquifer, AB, Canada. *Appl. Geochem.* **1991**, *6*, 405–418. [[CrossRef](#)]
19. Grazhdankin, D.V.; Podkovyrov, V.N.; Maslov, A.V. Paleoclimatic Environments of the Formation of Upper Vendian Rocks on the Belomorian-Kuloi Plateau, Southeastern White Sea Region. *Lithol. Miner. Resour.* **2005**, *40*, 232–244. [[CrossRef](#)]
20. Rozanov, A.Y.; Bessonova, V.Y.; Brangulis, A.P.; Giants, V.A. *Paleogeography and Lithology of the Vendian and Cambrian of the Western Part of the Eastern European Platform*; Nauka: Moscow, Russia, 1980.
21. Barnes, C.E.; Cochran, J.K. Uranium geochemistry in estuarine sediments: Controls on removal and release processes. *Geochim. Cosmochim. Acta* **1993**, *57*, 555–589. [[CrossRef](#)]
22. Mikhailov, B.M. *The Forecast of the Supergene Zones at Solid Minerals*; VSEGEI: St. Petersburg, Russia, 1998.
23. Shore, G.M.; Starchenko, V.V.; Myronyuk, E.P.; Kudryavtsev, V.E.; Radyukevich, N.M.; Alekseenko, V.D.; Shipov, R.V. *Requirements to Maps of the Ore-Bearing of the Supergene Zones*; VSEGEI: St. Petersburg, Russia, 2005.
24. Goretsky, G.I. *Alluvium of the Great Anthropogenic Paleorivers of the Russian Plain*; Nauka: Moscow, Russia, 1964.
25. Kashtanov, S.G. The geological data of Pliocene age of the Kazanka and Sviyaga rivers valleys. *Uchenye Zap. Kazan. Univ.* **1954**, *114*, 155–163.
26. Kashtanov, S.G. New data to the history of the Paleo-Kama. *Dokl. Earth Sci.* **1956**, *106*, 708–711.
27. Malov, A.I. Water-Rock Interaction in Vendian Sandy-Clayey Rocks of the Mezen Syncline. *Lithol. Miner. Resour.* **2004**, *39*, 345–356. [[CrossRef](#)]
28. Zverev, V.P.; Malov, A.I.; Kostikova, I.A. Geochemical state groundwater of the active water exchange zone at the Lomonosov diamond deposit. *Geocology* **2005**, *4*, 298–303.
29. Cheng, H.; Edwards, R.L.; Hoff, J.; Gallup, C.D.; Richardsc, D.A.; Asmeromd, A. The half-lives of uranium-234 and thorium-230. *Chem. Geol.* **2000**, *169*, 17–33. [[CrossRef](#)]

30. Head, M.J.; Gibbard, P.L. Early-Middle Pleistocene transitions: Linking terrestrial and marine realms. *Quat. Int.* **2015**, *389*, 7–46. [[CrossRef](#)]
31. Azzaroli, A.; De Giuli, C.; Ficarelli, G.; Torre, D. Late pliocene to early mid-pleistocene mammals in Eurasia: Faunal succession and dispersal events. *Palaeogeogr. Palaeoclimatol. Palaeoecol.* **1988**, *66*, 1–143. [[CrossRef](#)]
32. Markova, A.K.; Vislobokova, I.A. Mammal faunas in Europe at the end of the Early—Beginning of the Middle Pleistocene. *Quat. Int.* **2016**, *420*, 363–377. [[CrossRef](#)]
33. Muttonia, G.; Giancarlo Scardiab, G.; Kentc, D.V. Human migration into Europe during the late Early Pleistocene climate transition. *Palaeogeogr. Palaeoclimatol. Palaeoecol.* **2010**, *296*, 79–93. [[CrossRef](#)]
34. Ehlers, J.; Astakhov, V.; Gibbard, P.L.; Mangerud, J.; Svendsen, J.I. GLACIATIONS | Middle Pleistocene in Eurasia. In *Reference Module in Earth Systems and Environmental Sciences, Encyclopedia of Quaternary Science*, 2nd ed.; Elsevier: Amsterdam, The Netherlands, 2013; pp. 172–179.
35. Lisitsyn, A.P. (Ed.) *The White Sea System*; Nauchn. Mir: Moscow, Russia, 2010. (In Russian)
36. Molodkov, A.N.; Bolikhovskaya, N.S. Long-term palaeoenvironmental changes recorded in palynologically studied loess-palaeosol and ESR-dated marine deposits of Northern Eurasia: Implications for sea–land correlation. *Quat. Int.* **2006**, *152*, 37–47. [[CrossRef](#)]
37. Glaznev, V.N.; Kukkonen, I.T.; Rajewsky, A.B.; Ekinen, J. New data on the heat flow in the central part of the Kola Bay. *Dokl. Earth Sci.* **2004**, *396*, 102–104.
38. DePaolo, D.J.; Maher, K.; Christensen, J.N.; McManus, J. Sediment transport time measured with U-series isotopes: Results from ODP North Atlantic drift site 984. *Earth Planet. Sci. Lett.* **2006**, *248*, 394–410. [[CrossRef](#)]
39. Malov, A.I.; Kiselev, G.P.; Rudik, G.P. Uranium in the groundwater of the Mezen Syncline. *Dokl. Earth Sci.* **2008**, *421*, 965–968. [[CrossRef](#)]



© 2017 by the author. Licensee MDPI, Basel, Switzerland. This article is an open access article distributed under the terms and conditions of the Creative Commons Attribution (CC BY) license (<http://creativecommons.org/licenses/by/4.0/>).